Receiver Operating Characteristic Analysis

Application to the Study of Quantum Fluctuation Effects in Optic Nerve of Rana pipiens

THEODORE E. COHN, DANIEL G. GREEN, and
WILSON P. TANNER, JR.

From the School of Optometry, University of California, Berkeley, California 94720, the Vision Research Laboratory, University of Michigan Medical Center, Ann Arbor, Michigan 48104, and the Department of Psychology, University of Michigan, Ann Arbor, Michigan 48104

ABSTRACT Receiver operating characteristic (ROC) analysis of nerve messages is described. The hypothesis that quantum fluctuations provide the only limit to the ability of frog ganglion cells to signal luminance change information is examined using ROC analysis. In the context of ROC analysis, the quantum fluctuation hypothesis predicts (*a*) the detectability of a luminance change signal should rise proportionally to the size of the change, (*b*) detectability should decrease as the square root of background, an implication of which is the deVries-Rose law, and (*c*) ROC curves should exhibit a shape particular to underlying Poisson distributions. Each of these predictions is confirmed for the responses of dimming ganglion cells to brief luminance decrements at scotopic levels, but none could have been tested using classical nerve message analysis procedures.

INTRODUCTION

Receiver operating characteristic (ROC) analysis provides a framework for testing hypotheses concerning measured neuronal activity (see Appendix). In this paper, ROC analysis is employed to test implications, not otherwise testable, of the hypothesis that only quantum fluctuations limit the ability of retinal ganglion cells to signal luminance change information.

Quantum Fluctuations

The earliest statement that quantum fluctuations should set the limit on the detectability of luminance change for a visual system is due to deVries (1943) and to Rose (1948). Since the number of arriving quanta in a fixed space/time interval obeys a Poisson probability distribution, a slight change in that number, as would occur for a luminance increment or decrement, might be

impossible to distinguish from the naturally occurring fluctuations of that number. The variance of a Poisson distribution equals the mean, so that the luminance change that satisfies the requirement that it be just detectable increases as the mean is increased.

deVries and Rose independently arrived at the quantitative statement that the just-detectable luminance increment, E, should rise as the square root of the background luminance, B. That is,

$$E = KB^{1/2}. \quad (1)$$

This is called the deVries-Rose law. In the frog, as is the case in other animals, the deVries-Rose law only holds over a very small range of low backgrounds (ten Doesschate, 1958). More commonly, increment threshold is independent of background (near absolute threshold) and rises proportionally to background (Weber's law) at higher levels (ten Doesschate, 1958; Maturana et al., 1960). While the deVries-Rose law indisputably represents an ideal towards which evolutionary pressure may push (Barlow, 1964), data consistent with the law provide only weak support because they can be alternatively explained as a region of transition in the threshold versus background curve between absolute threshold and the Weber law behavior at higher levels.

In vertebrates, the best evidence of quantum fluctuation effects comes from the studies of Barlow and Levick (1969 *a*, *b*) concerning "on-center" cat retinal ganglion cells. For weak stimuli at low adaptation levels the number of extra action potentials elicited is proportional to the number of quanta in the stimulus (Barlow and Levick, 1969 *a*). In addition, the variability of the maintained discharge, expressed as the mean spike count in a fixed period divided by the variance, decreases with increasing adaptation level (Barlow and Levick, 1969 *b*). This is what would be expected of a quantum fluctuation limited system although it is certainly explainable in other ways (see Results below).

Fain's recent evidence (Fain, 1975), however, suggests that at low light levels toad retinal receptors are functionally dependent. Perhaps the purpose of this mechanism is to smooth over the variability due to quantum fluctuations. This weighs against the possibility of finding manifestations of quantum fluctuations later in the system.

The strongest direct evidence that quantum fluctuations explain threshold visual performance comes from experiments on invertebrates. The presence of quantum bumps (Yeandle, 1958; Ratliff et al., 1968) is suggestive and the experiments of Reichardt and colleagues (1966) which showed that measured variability matched the variability expected due to the rate at which photons were incident, leave little room for alternative explanations.

A few psychophysical experiments provide indirect evidence that favors the

quantum fluctuation hypothesis. For example, it is presumed that the Poisson variability of a stimulus at absolute threshold is manifest in frequency-of-seeing curves (Hecht et al., 1942) and in stimulus rating (Sakitt, 1972). Also, recent psychophysical studies, based on predictions similar to those tested in the present paper, suggest that under carefully selected conditions the size of the foveal increment threshold is determined by quantum fluctuations (Cohn, 1974, 1975[1]).

Several features of the problem of investigating quantum fluctuation effects make new investigations difficult. First, fluctuations mean noisiness of measurement so that large experiments are essential to discover the effect of the Poisson features of the stimulus. Second, since the nervous system is not necessarily linear one cannot expect to find a Poisson process at the level of the ganglion cell.

What is also needed is a way to assay nerve messages that sacrifices neither objectivity nor reliability in the face of randomicity. The procedure cannot be influenced by unknown nonlinearities of the system under study and it must be embedded in a theoretical framework that provides a richer set of predictions than the laws relating sensitivity to background (deVries-Rose), to area (Piper), and to duration (Piéron). Classical procedures of nerve message analysis do not satisfy these objectives. ROC analysis as applied to physiological measurements (Cohn, 1969) is a method of analyzing nerve messages which, when used in conjunction with the theory of signal detectability, allows tests of new predictions of the quantum fluctuation theory. The purpose of this paper is to describe such tests on class IV (dimming detector) optic nerve fibers of *Rana pipiens*.

Terminology

In this paper, some terms will be used that have been defined in the Appendix. These include: detectability, signal, noise, stimulus, measured distribution, underlying distribution, ROC curve, hit rate, false alarm rate, efficiency, and quantum efficiency. Often their colloquial use of misleading in the present context, so definitions should be consulted by the reader unfamiliar with them.

Predictions

In the Appendix (section D) the ideal detectability of a luminance signal obscured by additive gaussian noise is formulated in the framework of the theory of signal detectability. d'_e, the index of detectability of a signal, is derived to be proportional to signal luminance change, E, and inversely proportional to the square root of the noise variance. If quantum fluctuations, not added gaussian noise, obscure the luminance signal then Poisson distri-

[1] Cohn, T. E. 1975. Quantum fluctuation limit in foveal vision. *Vis. Res.* In press.

butions, not gaussian distributions, describe the problem. However, the cases are so similar that the latter may be used as an approximation for the former (Tanner and Clark-Jones, 1960). Suppose that the total number, N, of photons received from a background, B, for a duration, T, and over an area, A, is distributed as Poisson with mean BAT if no signal is sent and mean $(B - E)AT$ if a decrement signal is sent. Since Poisson distributions may be approximated as gaussian, and since the standard deviations of the two distributions ($\sqrt{BAT}$ and $\sqrt{(B - E)AT}$) can be considered approximately equal, the decision problem is represented by two nearly gaussian distributions with nearly equal standard deviation, $(BAT)^{1/2}$ and difference of means, EAT. As described in the Appendix, detectability, d'_e, in the gaussian equal-variance case is the separation of means divided by the common standard deviation. Therefore, in the Poisson case one has the following approximation:

$$d'_e = \frac{EAT}{(BAT)^{1/2}}. \tag{2}$$

Eq. 2 expresses the predicted ideal performance for this stimulus situation.

Eq. 2 involves an approximation which tends to underestimate d'_e. For decrements less than 75% of the background the maximum error in d'_e is 26% for backgrounds as low as four photons per integrating time per area. A more complete description of errors may be found in Table II in the Appendix.

For an observer that is ideal except that it catches only a fraction, F, of the incident quanta,

$$d'_e = \frac{FEAT}{(FBAT)^{1/2}}. \tag{3}$$

The deVries-Rose law, relating luminance change, E, for a fixed level of performance (d'_e = constant) to background luminance, B, may be seen to be a special case of the formulation presented in Eq. 3. So too are Piper's law relating E to area, A, and Piéron's law relating E to duration, T.

METHODS

Fig. 1 shows a schema of the experimental apparatus. Most of the experiments were performed on unanesthetized frogs. Frogs were cooled in crushed ice before and during surgery (Kaplan, 1967). The cooled frog was restrained and the sciatic and Vth cranial nerves were sectioned bilaterally.

The right optic tectum of the frog was exposed for microelectrode penetration. A small hole in the bone over the left tectum was made for the Ag-AgCl indifferent electrode. The microelectrodes used (Gesteland et al., 1959) were Indium-Wood's Metal filled glass micropipettes with 5–10 μm gold balls at the tips, plated with platinum black.

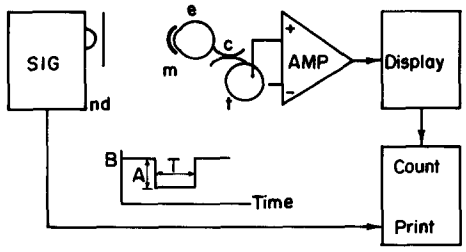

FIGURE 1. Schematic diagram of the experiment. Light from the signal generator, SIG, can be attenuated by neutral density filters, nd, and shines on diffusing plate, *m*, immediately in front of the frog's left eye, *e*. In a given run, the luminance of the diffusing plate is maintained at a fixed level except for occasions on which a signal occurs. The optic nerve from the left eye crosses completely at the chiasm, *c*, and projects to a layer near the surface of the right optic tectum, *t*. The head stage amplifier, AMP, monitors the potential difference between the microelectrode (+ input) in the dimming cell layer, and the indifferent electrode (− input) positioned over the left tectum. The output of this amplifier is displayed, and the display apparatus controls a spike-counting and count-printing operation. The identity of the signal used on a given trial is also recorded by the printer. Inset shows intensity versus time for a pulse decrement signal. Amplitude (A), duration (T), and background (B) were variable.

An hydraulic system was used to advance and retract the electrode. The electrode potentials were led to an FET-input differential amplifier (KM-47C, K and M Electronics, Northvale, N.J.; and see Cohn, 1969, p. 11 for circuit details) with 10^{12}-Ω input impedance and adjustable negative capacity compensation. The two outputs of the FET head-stage were led to the differential vertical amplifier of a dual beam, dual time base oscilloscope. The lower beam of the oscilloscope was used to monitor individual action potentials so as to minimize the likelihood of multicell recording. Each action potential detected by the lever trigger circuitry of the oscilloscope initiated a standard square pulse of fixed amplitude and duration. Such pulses were used to produce dot pattern displays (Wall, 1959) on a storage oscilloscope and were also counted as described below. A diffuser was placed immediately in front of the frog's left eye so as to produce uniform retinal illumination. The preparation was shielded from all other sources of light. A current-feedback-controlled (Green, 1969) 6-W fluorescent lamp (F6T5-CW) was used as background and signal source. The correlated color temperature of the lamp was approximately 3,800°. A 1-cm^2 area of the lamp was imaged on the diffuser using a 2.3-cm diameter lens placed 30 cm from the lamp. No other light could reach the diffuser. The luminance at the diffuser was set to a steady level which was controlled by electronic means as well as by neutral density filters placed between the lamp and the diffuser. Luminance measurements were made at the diffuser with an SEI photometer (Salford Instruments, England) calibrated using the certified standard source of a McBeth Illuminometer (Leeds & Northrup Co., North Wales, Pa.). The signals used were pulse decrements of the fixed adapting level with duration variable from 4 to 50 ms and amplitude modulation variable from 0 to 90%. (The frequency characteristic of the light controller was nearly flat [±3 dB] from DC to 3,000 Hz, so that rise and fall times for pulse decrements were less than 1 ms.) In addition, lamp intensity was monitored using an RCA type 934 vacuum phototube (RCA Electronic Components, Harrison,

N.J.), was found to be linear for sinusoidal modulation depths ranging to 92%. The fundamental experiment involved the presentation to the light-adapted frog of either a dimming signal or no signal on each of many trials.

Action potentials were counted during 0.7 s after the stimulus presentation. Pulse number distributions were generated from the recorded spike counts, processed to yield ROC curves as described in the Appendix, and then d'_e was computed, also as described in the Appendix.

RESULTS

Two types of experiments were performed. In the first, d'_e was estimated from spike count distributions for various size luminance decrements at a given background. The decrement energy was varied by varying duration from 1 to 45 ms. In the second type of experiment, background was varied by the introduction of neutral density filters between the lamp and the diffusing plate. A neutral density filter attenuates signal luminance and background luminance in the same way, because both signal and background are produced by the same lamp.

Detectability and Luminance Change

In order to test the hypothesis that d'_e is proportional to the size of a luminance change when duration is varied it is important first to show that stimulus duration is less than the integrating time of the ganglion cell. Fig. 2 shows distribution of spike count for a 25% decrement of the background lasting 100 ms and for a 50% decrement lasting 50 ms. 800 trials were taken for each stimulus over a period of 8 h. Both stimuli produce responses well above the spontaneous rate of about two spikes per counting interval. The distributions are similar both in mean and variance. The χ^2 test reveals no significant differences ($\chi^2 = 11.7$, df = 12). These data are consistent with

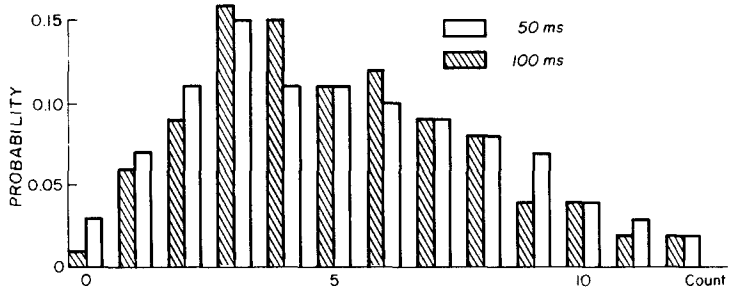

FIGURE 2. Distributions of spike count in 0.7-s interval after presentation of 100-ms decrement of 45% modulation and 50-ms decrement of 90% modulation. Ordinate: Relative frequency. Abscissa: Number of spikes counted. The maintained discharge for this cell was about 2 spikes/0.7 s. The response distributions appear to be nearly identical. $\chi^2 = 11.7$ (df = 12) is not significant. These data allow the conclusion that this cell has an integrating time of at least 100 ms. Backgrounds at 0.34 cd/m². Unit: II-68-b.

the assertion of ten Doesschate (1958) that the frog dimming cell has an integrating time of at least 60 ms. The larger value reported here is probably due to the lower adaptation levels used in these experiments.

The above test was performed at the highest adaptation level that was used in subsequent experiments so it was presumed that stimuli of lower duration (45 ms and less) would satisfy the assumption of perfect temporal integration at all adaptation levels. ROC curves were measured for fixed modulation, variable duration decrements in most experiments.

Fig. 3 shows ROC curves for two decrement stimuli. They are fit with Gaussian ROC curves for which the values of d'_e stand in the same ratio as the durations of the two stimuli. This result is consistent with the prediction of Eq. 2.

Fig. 4 *a* plots d'_e versus signal energy for this cell and for two others. Lines passing through the origin are fit by eye to the data points. Four other cells, tested in experiments with fewer trials showed consistent results. These results extend the finding of Fitzhugh (1957) who showed that d'_e for increments is nearly linear with the size of the increment, and they are consistent with psychophysical findings in humans (Cohn et al., 1974).

In Fig. 4 *b*, the mean response (additional spikes above maintained level in 700 ms) is plotted versus signal energy for the three cells whose data are shown in Fig. 4 *a*. Two of these stimulus-response functions depart from linearity in a consistent way. They show that the response for small signals,

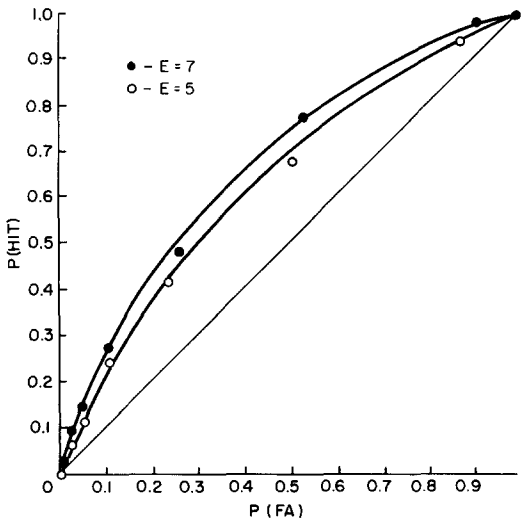

FIGURE 3. ROC curves for two different duration dimming signals, linear paper. Upper curve for 38.5 ms, 40% dimming of 0.034 cd/m² background. Lower curve for 27.7-ms signal. d'_e is 0.63 and 0.44, respectively. 300 trials per distribution for each curve. Unit IV-36-a.

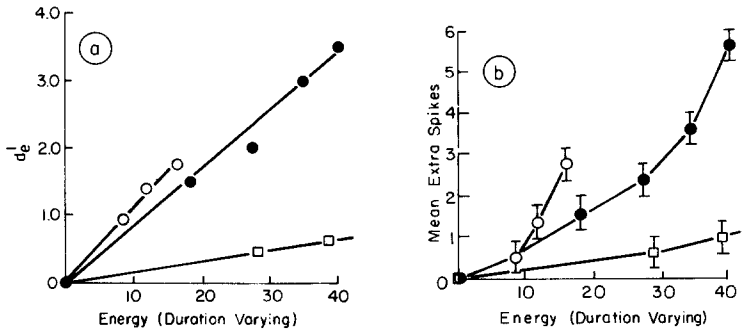

FIGURE 4. (*a*) Detectability, d'_e, of dimming signal versus energy. Ordinate: d'_e. Abscissa: Signal energy, equal to product of dimming modulation times duration. (Duration varying up to 40 ms.) Three different cells represented. Upper two curves for background of 0.34 cd/m². Lower curve for background of 0.034 cd/m². Units: IV-55-a, IV-70-a, and IV-36-a. (*b*) Ordinate: Average number of spikes exceeding maintained rate counted in 0.7 s interval after signal. Arbitrary units arranged so that point for highest signal plotted at same ordinate as in 4 *a*. Abscissa: Same as in 4 *a*. ± 2 SE bars plotted. Two of the cells clearly show an accelerating function. No conclusion can be drawn from the third.

measured as an increment of spikes upon the maintained rate, is an accelerating function of signal energy, not a linear one. No conclusion can be drawn for the third cell. For large signals we find as did Barlow and Levick (1969 *a*) that the response mechanism saturates. But d'_e remains linearly related to signal energy (an example appears in Fig. 5 below). Both results illustrate an important feature of ROC analysis; even though the function relating the input to the output of the system under study is nonlinear, detectability (d'_e) may be linear with signal energy. If so, it means (Birdsall, 1966) that the variability in the nerve message originates distal to the nonlinearity.

If there had been a linear relation between stimulus and response, as Barlow and Levick (1969 *a*) showed for a range of signals in on-center cat retinal ganglion cells, and if the variance of pulse number distributions did not depend upon the size of the luminance change signal, as Fitzhugh (1957) suggested, then d'_e would be linear with average response and it would suffice to measure the latter. Using ROC analysis to define a sensitivity measure would be superfluous under those conditions.

In the urethane anesthetized frog, spontaneous activity is so low that the spike count distribution for no signal is statistically trivial (Cohn, 1969). Then ROC curves for all detectable stimuli produce $d'_e = \infty$ because signal and no-signal distributions have little or no overlap. Therefore, the hypothesis of a linear d'_e versus E function cannot be tested. However, the hypothesis can be modified for test in the anesthetized animal as follows. Suppose that spike count distributions are compared for two different signals instead of for signal and for no signal. The prediction becomes $d' = C\Delta E$ where ΔE is the

difference of energy between the two signals. In other words, discrimination between stimuli is also predicted to be linear with energy. Fig. 5 shows d'_e versus ΔE for an experiment in which decrement amplitude, not duration, was varied. This finding, that d'_e is linear with difference energy in a discrimination situation, was confirmed in seven other cells. It is implicit in the findings of Fig. 4.

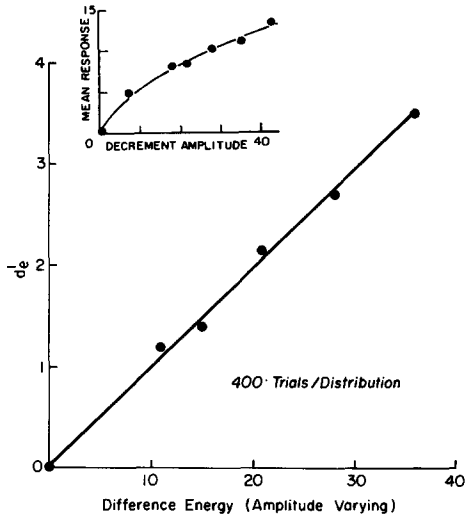

FIGURE 5. Detectability for discrimination between signals. Ordinate: d'_e estimated from pairs of spike count distributions for different size energy difference, using bootstrap procedure (details in appendix). Abscissa: Difference of energy between signals. Energy adjusted by varying duration. Line is fit by eye to pass through origin. It represents the prediction that detectability is linear with difference energy. Inset: Estra spikes (ordinate) as a function of energy of dimming signal (abscissa). Smooth curve drawn to illustrate saturation-type function. Urethan anesthetized preparation. No spontaneous activity. Background at 0.34 cd/m^2. Unit: IV-92-a.

Detectability and Background

The second fundamental prediction of the quantum fluctuation hypothesis is that detectability (d'_e) should vary inversely with the square root of background. It is instructive to contrast this prediction with Weber's law, that a fixed percentage decrement produces a constant response independent of background (e.g., that d'_e varies inversely with background for E fixed, or d'_e is a constant for E/B fixed). Fig. 6 shows dot pattern displays in which each dot represents a spike. The horizontal axis is time, and the vertical axis is changed slightly by a trial counter so that each trial produces a separate dot pattern.

In each of the four displays, the upper half is for 40 trials with a small decrement (about 10% of background) and the lower half is for 40 trials with

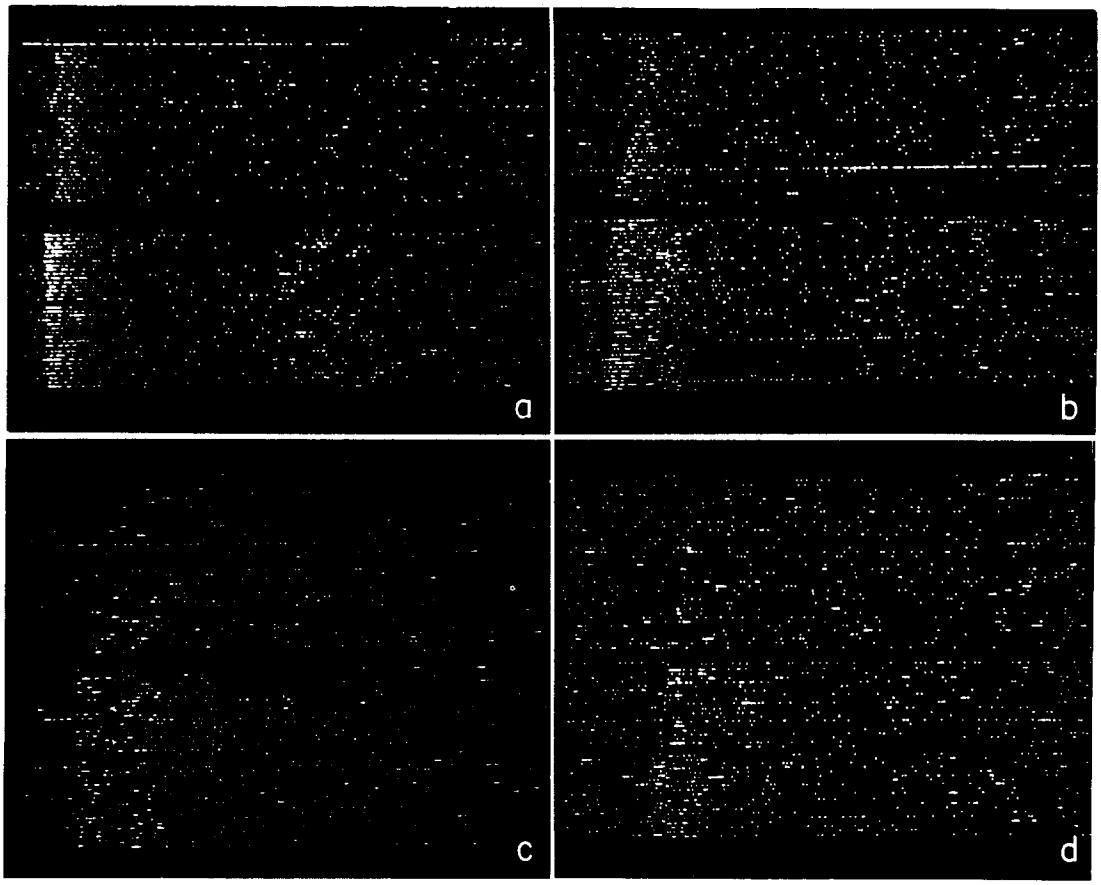

FIGURE 6. Dot pattern displays (Wall, 1959) at different adaptation levels. Each horizontal trace is for a different trial and each dot shows the occurrence of a spike. Total horizontal trace represents 0.5 s after signal. There are 40 traces for a small signal (upper half of each panel) and 40 traces for a large signal (lower half), which were alternated in the experiment. In panels *a* through *d*, the ratio of decrement to background is fixed. Background lowered by the introduction of neutral density filters as follows: (*a*) 0.34 cd/m^2, (*b*) 0.034 cd/m^2, (*c*) 0.0034 cd/m^2, (*d*) 0.00034 cd/m^2. As background is decreased, responses show longer latency, fewer spikes, and more variability. Weber's law clearly does not hold because it would predict identical responses at each background since the ratio of decrement to background is fixed. Unit III-92-1.

a large decrement (about 30% of the background). The two stimuli were alternated. The displays from *a* through *d* represent experiments at backgrounds of 4, 3, 2, and 1 log units, respectively (4 corresponds to 0.34 cd/m^2). Firstly, spontaneous activity (which can be assessed at the far right of each trace, around ½ s after the stimulus presentation and after the response) is roughly the same at all backgrounds. The response is most vigorous in *a* showing a primary response of high pulse frequency about 0.1 s after the

stimulus onset, followed by a second frequency increase perhaps 0.2 s later for the larger stimulus. In *b*, the secondary response is almost completely obscured by spontaneous activity, and the primary response has increased latency and duration but decreased spike count. This progression continues through *c* to *d*. Therefore, a stimulus that is a fixed percentage decrement of the background does not produce the same response at all backgrounds so that Weber's law clearly fails to hold. In fact, detectability of a fixed percentage decrement increases for increasing background which matches qualitatively the quantum fluctuation prediction (it must be remembered that E, the numerator of Eq. 1, increases linearly with B because of the stimulus source configuration so that $E/B^{1/2}$ goes up with background). Over this range of adaptation levels, frog pupil size as measured with an infrared closed-circuit television pupillometer, (Green and Maaseidvaag, 1967) did not change.

On the basis of studies by Liebman and Entine (1968) showing that over 90% of the frog retinal photopigment is rhodopsin and by Donner and Reuter (1968) showing that cones do not respond at backgrounds below 10^{12} quanta (615 nm) $s^{-1}mm^{-2}$ (the backgrounds here are at most 10^{12} quanta (507 nm) $s^{-1}mm^{-2}$, see Discussion) it is likely that these responses monitored are from the scotopic system of the frog.

Quantitative tests of the quantum fluctuation hypothesis employing more trials were performed on 10 other cells. Fig. 7 shows log d'_es verus log B for 2 of the 10 cells. The straight line fitted to measured points has a slope of

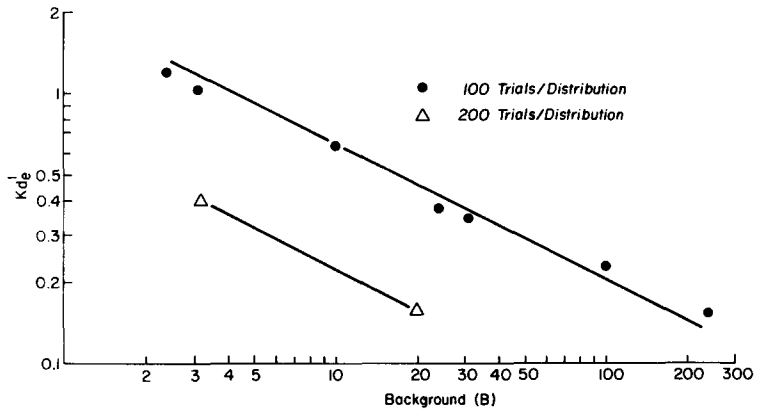

FIGURE 7. d'_e versus background, B, for two cells, log-log paper. In these experiments, background is varied with neutral density filters. At several values of background, E was also varied so as to keep measured d'_e near 1.0. The value of the ordinate is extrapolated to the d'_e that would have been achieved if E had been held fixed, on the assumption of a linear d'_e versus E function. Ordinate: d'_e. Abscissa: Background in arbitrary units. $B = 240$ corresponds to 0.34 cd/m² on diffusing plate. Lines of slope -0.5 are fitted by eye. They correspond to the deVries-Rose law, $d'_e = KB^{-1/2}$. Weber's law would be represented by a line of slope -1.0.

$-\frac{1}{2}$ which is the prediction of the quantum fluctuation hypothesis. Data from six others were consistent with these results. In the remaining two cells, tested at high background, the influence of background was stronger than shown above indicating that Weber's law (a line of slope equal to -1) may hold under conditions of still higher adaptation level.

An Alternative Model

Suppose that an internal noise source, (not quantum fluctuation noise) say at the level of the ganglion cells, obscured the dimming signal by adding a fixed variance to the membrane potential. If the noise were gaussian and if the incoming light signals were attenuated by a gain control mechanism whose attenuation varied as the square root of background then Eq. 2 describes the predicted variation of d'_e with E and B. So, while the data described above are consistent with the quantum fluctuation hypothesis they are consistent with at least one other idea that has nothing to do with quantum fluctuations. In order to separate these two hypotheses it is necessary to return to ROC analysis to find further predictions and an appropriate test.

If, instead of employing the gaussian approximation that leads to Eq. 2, one estimates d'_e for ROC curves plotted from Poisson distributions, Eq. 2 remains largely unchanged. However, the Poisson ROC curves are notably different from gaussian ROC curves for two reasons. Poisson ROC points are of the following parametric form:

$$\begin{aligned} P(\text{HIT}) &= \sum_{x=0}^{c} [\exp(-B + E)(B - E)^x] \div x! \\ P(\text{FA}) &= \sum_{x=0}^{c} [\exp(-B)B^x] \div x! \end{aligned} \tag{3}$$

Each integer value of c produces a different ROC point. When plotted on probability paper (Keuffel & Esser Co., Morristown, N. J., type 47 8062, see Fig. 5 *b* of the Appendix) these points fall on a straight line of slope greater than 1.0. Greater than unity slope reflects greater variance in the noise distribution than in the signal distribution. But it is not legitimate to connect these points by a straight line on probability paper. To assess an entire ROC curve from a set of achievable ROC points one connects those ROC points by straight line segments on linear paper. This is because an observer can, without any other information, randomize his use of the decision criteria leading to each obtained point and so operate somewhere on the line segment between them (see Birdall, 1966 for proof). Since single photons are indivisible the ideal observer cannot perform any better than is indicated by the interpolated line segment on linear paper. The interpolated line segment plots as a concave-upwards cusp on probability paper. Such cusps can occur only if (*a*) underlying distributions are discrete, and (*b*) measured distributions are

more fine grained (e.g., more than one extra action potential per extra photon). Therefore, points may, but need not, fall on cusps in the Poisson case. However, if underlying distributions are continuous as is the case in the alternative model described above, ROC points plotted from measured distributions (which may or may not be discrete) cannot fall on cusps. Fig. 8 illustrates ROC curve cusps.

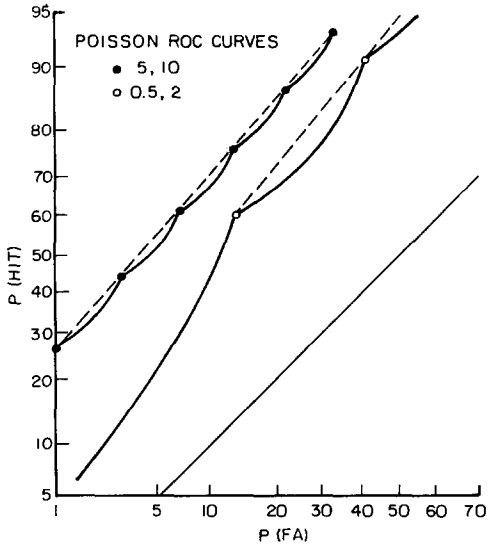

FIGURE 8. Theoretical Poisson ROC curves on probability paper. These curves are for Poisson distributions of means 0.5 and 2 (lower) and 5 and 10 (upper). Dashed curves are straight lines passing through ROC points. Slopes of these lines are greater than 1.0. Solid curves (cusps) show points interpolated by connecting adjacent ROC points plotted on linear paper with straight lines (Birdsall, 1966, p. 9). For the lower curve, the dashed line is terminated at the point (.605, .135) because that is the point that would be obtained if one or fewer photons were the criterion cutoff. The only lower cutoff leads to an ROC point at (0.0, 0.0). It is apparent that one would not expect to measure ROC cusps unless the quantum catch for the cell in question were close to one or two photons. Because of the inherent variability of ROC points, a measured ROC cusp should not lead to the inference of a low quantum catch without independent confirmatory evidence.

Figs. 9 and 10 display ROC curves from frog dimming cells to enable a test of these alternative hypotheses. Several of these curves are notable for the large number of trials used in obtaining them. With enough trials, a single ROC curve is sufficient to reject the internal added noise model. The curve of Fig. 10 is the best example of this. However, not all ROC curves were measured with this precision. In total, 36 of 58 curves had slopes greater than unity; 22 had slopes less than or equal to 1.0. The occurrence of ROC slope less than 1.0 is due not just to sampling error in the determination of pulse number distributions, but also to the fact that when a cell is held for only a short time the factors that cause it to be lost probably add variance to

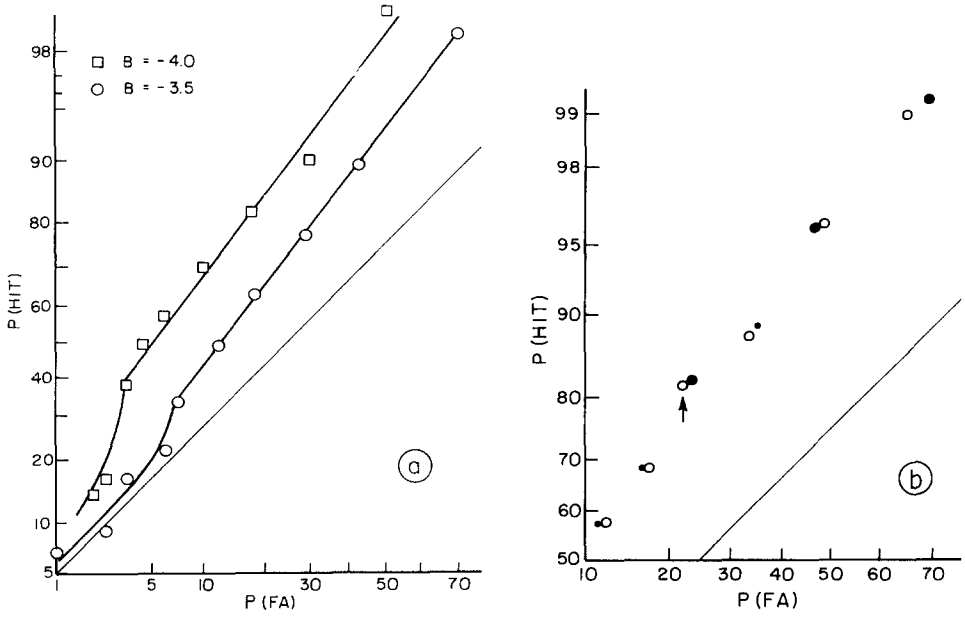

FIGURE 9. (*a*) ROC curves at low adaptation levels (probability paper). Ordinate: Hit rate. Abscissa: False alarm rate. Upper curve: Background at 0.017 cd/m², 150 trials per distribution. Lower curve: 0.0034 cd/m², 200 trials per distribution. These curves have slope greater than 1.0, and a cusp at the high spike count (e.g., low photon number) end of the curve. Unit IV-91-c. (*b*) ROC curve showing cusps. Ordinate: Hit rate. Abscissa: False alarm rate. Open circles are measured ROC points for Unit IV-77-a. Background = 0.0017 cd/m². Closed circles are for Poisson distributions with means 0.75 and 2.8 quanta, respectively. They were chosen so that ROC point for lowest possible cutoff (one spike) would match the measured point indicated by the arrow. Small filled circles are interpolated (using the rule that Poisson points may be connected by straight lines on linear paper) between theoretical points near the other measured points. This fitting procedure is intended as a guide; it is not justifiable to assert that the Poisson ROC curve is the only one that would fit the measured curve.

the measurement. That most cells exhibit ROC slope greater than unity is consistent with the finding of Barlow and Cohn (1971) on both "on"- and "off"-center cat retinal ganglion cells. They showed ROC curves with slope greater than 1.0 for decrements and less than 1.0 for increments.

With regard to cusps on ROC curves, the evidence is harder to obtain. While the curves derived from the largest number of trials and particularly those at low backgrounds all showed cusps, indicative of both a discrete input to the system and of a quantum to spike ratio less than 1.0 (see Figs. 9, 10), many ROC curves contained only three to five ROC points so that cusps would not be expected to appear. We know of no adequate statistical test to confirm the occurrence of cusps so their apparent occurrence must be con-

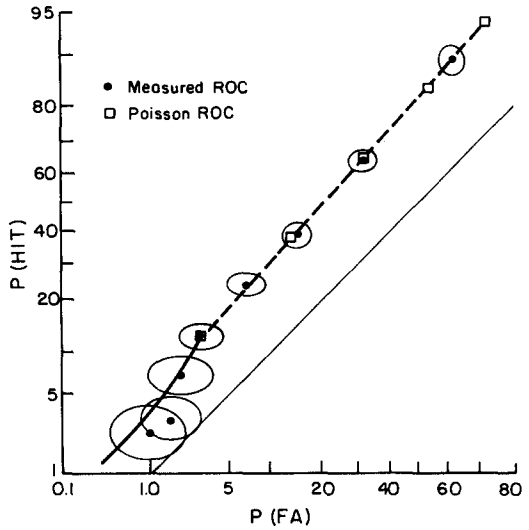

FIGURE 10. ROC curves on probability paper. Background, 0.0034 cd/m². 550 trials per distribution. Ellipses around experimental points represent 95% confidence limits on the assumption of binomial variance. Green and Swets (1966, p. 403) have pointed out that the binomial variance overestimates error due to the interdependence of the points. A theoretical Poisson ROC curve for distributions with means of 2.1 and 3.5 has been included for purposes of illustration (open squares, solid curve is cusp for interpolated points, slope of dotted portion is 1.1). Lower solid curve is chance line (slope = 1.0). Unit: IV-91-b.

sidered provisional. However, the inference of a quantum to spike ratio less than unity is consistent with a finding of Barlow et al. (1971) in the cat.

Evidence consistent with four predictions of the quantum fluctuation hypothesis has been presented: (*a*) d'_e is proportional to signal energy in a detection task and to the difference of signal energies in a discrimination task; (*b*) for a range of low backgrounds d'_e is inversely proportional to the square root of background; (*c*) on the average, ROC slope is greater than 1.0, and (*d*) ROC cusps occur, especially at low backgrounds, due to the discrete nature of the photon input. An internal noise model is described that explains the first two findings but not the last two.

DISCUSSION

We have concluded that the quantum fluctuation hypothesis, as formulated for tests using ROC analysis, predicts certain aspects of the behavior of frog retinal ganglion cells when luminance decrements are to be detected. Four separate predictions of the hypothesis were tested and confirmed. The first is a generalization of the deVries-Rose law that for fixed detectability, a decrement must be increased as the square root of background. The second pre-

diction was that detectability should be proportional to the size of the decrement. The third was that the ROC curve should exhibit greater than unity slope on probability paper. Finally, the ROC curve for a discrete valued input, such as would occur due to the corpuscular nature of light, should exhibit convex-downwards cusps. Except for a narrow version of the first, none of these predictions could have been formulated and tested with classical procedures of nerve message analysis.

The power of ROC analysis in making these deductions is illustrated with the following numerical analysis. Consider first the critical evidence that favors the view that quantum fluctuations are responsible for the observed variability. This evidence involves the slope of the ROC curve. A slope measured to be greater than 1.0 implies that variability of the underlying distribution when the signal was presented is less than that when the background alone was presented. But, the same pulse number (spike count) distributions show the opposite relation. Invariably the variance of the measured signal distribution is greater than that for the no-signal measured distribution.

For example, the slope of the ROC curve of Fig. 10 suggests that the variance of signal and no-signal events is about $\sigma^2_{SN}/\sigma^2_N = 1/(1.1)^2 = 0.83$ while the variances of the measured pulse number distributions stand in a ratio of $3.8/2.3 = 1.65$. That is, the variance of the underlying signal distribution is less than that of the underlying noise distribution, just as Poisson statistics would predict. However, the variance of the measured (pulse number) signal distribution is larger than that of the measured noise distribution. This confirms the observation illustrated in Fig. 4 *b* of a nonlinear relation between photon count and pulse number. It shows how response size, which depends on an arbitrary choice of response scale (pulse number in this case) can lead to misleading inferences as to the statistical nature of underlying events. But ROC curves are independent of scale (to within a monotone transformation), so that inferences based upon ROC analysis are uninfluenced by both arbitrary choice of response scale and by nonlinearities. In this case, conventional statistical analysis procedures like computations of average response and response variance, would have failed to disclose that the data conform to the predictions of the quantum fluctuation hypothesis.

Spontaneous Activity

The nature and origin of spontaneous neural activity has been a question of great importance to neurophysiologists ever since it was discovered by Adrian and Matthews (1928). Jacobs (1972) has reviewed work in this area. Granit (1955) for example, has proposed that the purpose of spontaneous activity is to provide a means by which information may be signaled as positive or negative changes in firing rate. Our data are consistent with this idea, es-

pecially insofar as luminance increments tend to arrest the activity of the dimming cell. But why is the spontaneous activity variable?

Ratliff et al. (1968) recognized that the variability in the maintained discharge must limit the capacity of the nerve to carry information regarding external events. Barlow and Levick concur in this view (1969 *a*, *b*). Certainly, thermally caused membrane potential fluctuations present an irreducible minimum variability of spike discharges (Verveen and Dirksen, 1965). Ratliff et al. (1968) were led to the view, however, that the largest component of variability in *Limulus* eccentric cell discharge was initiated in the photoexcitatory process because the variability changed in response to various adapting conditions. This is consistent with our evidence that the variability of frog dimming cell discharge is due to quantum fluctuations. We have shown that the variability at a given adaptation level depends upon the signal used, the bigger the dimming signal the *less* variable the underlying distribution of events in the event that the signal had occurred. Thus, in our view, spontaneous activity is a coding of on-going photoisomerizations due to the background, its variability arising from the inherent fluctuations due to the corpuscular nature of light. Quantum fluctuations may not be responsible for variability at levels of adaptation higher than those we measured because eventually the relative variability due to quantum fluctuations (which decreases as $B^{1/2}$) would be expected to become less than thermally induced membrane potential fluctuations.

Quantum Efficiency

If it is true, as suggested by the data, that quantum fluctuations limit the detectability of luminance decrements, it should be possible to calculate the quantum efficiency, F, of dimming cells. F is defined as the fraction of available photons that give rise to the nerve signals that are monitored. There are two ways to make this computation, and they must be reconciled with the physical estimate of the number of photons available in the receptive field of the cells under test. The first method makes use of the relative size of decrement and background and the detectability measured. In the experiment the results of which appear in Fig. 10, for example, the decrement was a 40% modulation of the background and the detectability, d'_e, of this stimulus was about 0.8. Knowing the number of photons available to the frog one can use these data to calculate F.

The number of quanta available to the frog in this experiment can be approximated as follows: it is accepted that rods of *Rana pipiens* which contain rhodopsin (Crestitelli, 1958; Liebman and Entine, 1967) mediate responses at these adaptation levels, and it is assumed that a calculation applicable in the human (LeGrand, 1968) suffices in frog with changes appropriate to the dif-

ferences in size for the two eyes. Assuming (*a*) 7-mm^2 pupil, (*b*) the retina lies 4 mm from the principal point, (*c*) 10% of quanta passing pupil are absorbed in photopigment,[2] and (*d*) human scotopic sensitivity; approximately 4×10^3 quanta are absorbed at the retina in a 1-mm^2 receptive field. While there is considerable uncertainty attached to this number owing to the assumptions involved, its implications are worth pursuing. From Eq. 3 relating detectability, d'_e, to number of photons decremented, EAT, from a steady level, BAT

$$d'_e = \frac{(FEAT)}{(FBAT)^{1/2}},$$

where BAT is 4×10^3 quanta and $EAT = 1.6 \times 10^3$ quanta, F is calculated to be 2×10^{-3}.

This is a lower limit on quantum efficiency. It assumes that the eye receiver integrates for no more than the signal duration. However, the spike counter counts for 0.7 s which leads to an upper limit for BAT of 6.6×10^4 quanta. EAT remains 1.6×10^3. Then, using Eq. 4 again $F = 1.65 \times 10^{-2}$, which is an upper limit. It must be pointed out that F is interpreted as the fraction of photons available *at the retina* which are used in the task. The overall quantum efficiency has been assumed (above) to be lower by a factor of 10 due to losses in the ocular media and to inefficient quantum catching in the retina.

Another way to estimate quantum efficiency is by fitting the slope of a measured ROC curve with that of an ROC curve computed from Poisson distributions. The Poisson distributions must satisfy certain constraints. First, the mean of the signal distribution can be no more than 70% less than that of the no-signal distribution since that is the percent modulation of the decrement during its 42.5-ms duration. The ROC curve which matches $d'_e = 0.8$ and has the same slope as the measured curve is for Poisson distributions of means 2.1 and 3.5, respectively (see Fig. 10). Thus, 3.5 is a lower limit for $FBAT$; with $BAT = 4 \times 10^3$, $F = 0.9 \times 10^{-3}$. The upper limit of $FBAT$ is found by observing that the integrating time of the entire system could be no more than the counting period, which was 700 ms.

If so, the modulation of the background, expressed as a percent of the

[2] The figure of 10% for human vision is probably a lower limit for the case of *Rana pipiens*: Kennedy and Milkman (1956) showed virtually no lens absorption above 440 nm. 92.8% of photoreceptors in *R. pipiens* are red rods (Liebman and Entine, 1968) containing rhodopsin (Crescitelli, 1958; Liebman and Entine, 1967) of optical density 0.7–0.8 (Liebman and Entine, 1968). From the estimate of Denton and Wyllie (1955) that red rods occupy 59% of the surface area of the retina of *R. temporia* and presuming corneal reflection to be negligible, it follows that about 50% of photons incident at the cornea are absorbed in photopigment. The corresponding figure from Hecht et al. (1942) for humans is 10%. Denton and Pirenne (1954) assumed a lower limit of 10% and an upper limit of 100% for *Xenopus laevis*.

total quantum catch, could be as little as, but no less than 4.2%. In this case, the Poisson ROC curve which has the same d'_e as that of the measured curve is for distributions with means of 362 for the signal and 377 for the background. Then $BAT = (700 \text{ ms}/42.5 \text{ ms}) \times 4 \times 10^3 = 6.6 \times 10^4$ and so $F = FBAT/BAT = 377/6.6 \times 10^4 = 5.7 \times 10^{-3}$.

However, the fit of the curve for distributions of 377 and 362 quanta is much worse than that for curves of lower Poisson mean because the slope of this curve is 1.02, significantly less than that of the measured curve. Thus, the quantum efficiency calculated by the second method is between 5.7×10^{-3} and 0.9×10^{-3} with greater reliability supposed for the lower estimate.

In summary, two independent methods of computing quantum efficiency suggest that between 0.1 and 1.6% of the photons received at the retina in the receptive field of the cell are used in the task. These low values do not necessarily imply an inefficient phototransduction process. Possibly the dimming ganglion cell receives input from only 1% of the receptors in its very large receptive field. This anatomical suggestion is plausible since dimming cells code no detail information (Maturana et al., 1960).

SUMMARY

(*a*) We have measured pulse number distributions from recorded activity of dimming ganglion cells of *Rana pipiens* for decrement stimuli of various sizes on several fixed adapting levels. The quantum fluctuation hypothesis of luminance change detection was formulated in a framework called ROC analysis in order to test its several predictions. (*b*) ROC curves were calculated from pulse number distributions obtained by measuring single cell activity with and without dimming signals. (*c*) Signal detectability, d'_e, was estimated from ROC curves. (*d*) Detectability, d'_e, is linear with decrement amplitude times duration. (*e*) Values of d'_e decrease in proportion to the square root of background luminance. (*f*) The slope of ROC curves on probability paper is usually greater than 1.0. (*g*) ROC curves often exhibit "cusps" indicative of both discrete value inputs (e.g., individual photons) to the system under study and of a quantum to spike ratio of less than 1.0. (*h*) All of these results (*d*, *e*, *f*, and *g*) are consistent with the predictions of the quantum fluctuation hypothesis. Two, *f* and *g*, are inconsistent with an added-internal-noise model. Except for *e*, a special case of the deVries-Rose law, they could not have been tested by classical data analysis methods because of a nonlinear relation between spikes measured and energy of decrement. (*i*) It is concluded that spontaneous activity codes irreducible changes of background light level, the variability of spontaneous activity reflecting the Poisson variability of the incident light. (*j*) The quantum efficiency of one cell, typical of the others, was calculated to lie between 1×10^{-3} and 1.6×10^{-2}. One way to explain this low value, which represents the fraction

of *absorbed* photons that are used, is to postulate that the ganglion cell receives input from only a small percentage of the receptors in its receptive field.

APPENDIX

ROC Analysis of Sensory Nerve Messages

Introduction

The study of sensory systems often involves experiments where the system under study is evaluated at the limits of its information-handling capabilities. Physiological responses measured in these experiments are difficult to evaluate owing to variability and to ongoing activity in the absence of stimuli. Useful innovations including averaging, histograms, and correlation techniques, have been introduced to cope with the statistical nature of responses (for a review see Moore et al., 1966). A major problem stems from the necessity for a subjective interpretation of the record by the experimenter when a sensitivity measure is desired. The latter difficulty has been cited frequently (Fitzhugh, 1957; Rosenblith, 1962; Barlow, 1965; Barlow and Levick, 1969 *a*) and is inextricably related to the statistical nature of physiological responses and to the existence and variability of ongoing activity.

Two particular attempts to alleviate the subjectivity problem are precursors to the method to be described here. Fitzhugh (1957) applied the theory of signal detectability to the problem of analyzing noisy nerve messages in cat retinal ganglion cells. He defined an objective sensitivity measure, d, in terms of the separation of the means of spike count frequency distributions measured both with and without a stimulus. Fitzhugh's d did not take account of the variance of the spike count distributions. Barlow and Levick (1969 *a*) argued that the variability of the maintained discharge should be expected to affect sensitivity and so devised an extension of Fitzhugh's analysis procedure which took that variability into account. Each of these methods is a specialized form of a general analysis procedure that was introduced as a combination of statistical decision theory and signal detection theory (Peterson et al., 1954).

The purpose of this Appendix is to describe ROC analysis for nerve messages (Cohn, 1969), a general method of analyzing measured nervous activity based upon the receiver operating characteristic (ROC curve) of the theory of signal detectability (Peterson et al., 1954). ROC analysis includes as special cases the data analysis procedures of Fitzhugh (1957) and of Barlow and Levick (1969 *a*). ROC analysis provides a procedure for defining an objective sensitivity measure but with fewer restrictive assumptions than the methods cited above. Coupled with the theory of ideal observers, ROC analysis provides the experimenter with means of testing new types of hypotheses concerning measured nervous activity. This Appendix discusses the manner in which ROC curves and the associated sensitivity measure, d'_e, are derived from frequency distributions of measured nervous activity.

Synopsis

First, the general experimental scheme for which this method is relevant will be described. Terminology is then defined in section B. Section C includes a method of

generating ROC curves from raw data, general properties of ROC curves, extracting measures of sensitivity and threshold, and statistical aspects of ROC curves and ROC curve parameter estimation. Finally, section D describes the use of the concept of the ideal observer in generating predictions for certain experimental situations.

Principle Underlying ROC Analysis

ROC analysis considers the experiment in terms of a communication channel analogy. Fig. 11 shows a block diagram of an experiment considered in this way. In the general case there are four components. A transmitter provides signals to the system under study, a measurement device monitors activity, and a receiver interprets the activity. In the examples to be used here, the transmitter provides decrement light signals to the frog on half of the trials of the experiment. (No signal occurs on the remaining trials.) The measurement device records extracellular activity of the frog dimming ganglion cell axon in the optic tectum. The receiver is a device that counts spikes for 0.7 s after the start of a trial. The frog is considered to be a communication channel through which information pertaining to the presence or absence of the decrement signal may flow. ROC analysis is based on the principle (Cohn, 1969) that the more accurately the receiver can draw inferences about the presence or absence of the signal the better must be the information-handling capability of the frog. ROC analysis assesses the decisions that the receiver *could have made* concerning the presence or absence of the signal based upon the information available in the measurement.

Assumptions

If certain assumptions are accepted, then it can be shown that the sensitivity measure, d'_e, derived from ROC analysis, is directly related to the Shannor-Weiner measure of information applicable to this communication channel (Cohn, 1969). Correspondence between sensitivity and the information measure (*a*) makes the ROC analysis procedure objective, (*b*) enables the investigator to make use of theories of optimal performance for comparison with measured performance, and (*c*) allows the investigator to gauge the influence of the particular choice of a receiver on his conclusions. Naturally, if the assumptions are violated, the objectivity, optimal performance comparisons, and ideas of receiver influence cannot be relied on. Accordingly, the assumptions implicit in the use of ROC analysis are outlined: (*a*) When a signal has been presented measured events are variable, and can be confused with events when no

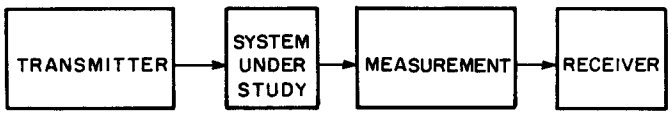

FIGURE 11. Communication channel analogy for the experiment. Signals, initiated by the experimenter, are transmitted to the system under study. Usually the measured effects due to a signal are compared to those due to no-signal transmission. If, using only the measurement, the receiver can correctly decide whether or not a signal has been presented, then the information-processing capability of the system under study can be quantified. ROC analysis assesses correlation between physical events at the transmitter and measured physiological events at the receiver.

signal has been presented. (This is what is meant by "threshold" conditions.) (*b*) The measurement on any trial is completely independent of the measurement on any other trial, and the system under study remains unchanged for all trials of an experiment. (*c*) The receiver that is used in a particular experiment has been designed so that its efficiency is not likely to be altered by changes in stimulus parameters, and so that neither it nor the measurement device contributes significantly to the variability in the measurements. (*d*) The "goodness" of hypothetical receiver decision-making involves preference for correct decisions over incorrect decisions. (*e*) The experiment can be represented as in Fig. 11 with one and only one pathway for information flow from transmitter, via the system under study, to the receiver.

(B) *Terminology*

The theory of signal detectability provides the means to assess the receiver as decision maker and subsequently to assess the system under study as information processor. The terminology of that theory as applied to the problem of analyzing sensory nerve messages is presented below. The following terms are defined: signal, stimulus, receiver, decision variable, criterion, hit rate, false alarm rate, likelihood ratio, detectability, efficiency, quantum efficiency.

SIGNAL The signal is the physical event produced at the transmitter. The word signal is not used interchangeably with the word stimulus.

STIMULUS The word stimulus is reserved for general use as in "stimulus conditions." It refers to all physical events influencing the system under study.

NOISE Noise is any process uncorrelated with the signal that contributes variance to the *measured distributions. External noise* is that which originates outside and *internal noise* that which originates inside the system under study.

RECEIVER A device that computes a unidimensional parameter of the measurement on each trial called the *decision variable.* (The extension of this technique to multidimensional decision variables will not be covered in this communication.)

DECISION VARIABLE The random variable computed by the receiver on each trial. Fox (cited in Tanner, 1961) has shown that the optimal decision variable for any situation where hits are preferred to false alarms is the *likelihood ratio.* In addition, Birdsall (1966) has shown that decisions based upon any monotone function of likelihood ratio are indistinguishable from those based upon likelihood ratio so any quantity monotone with likelihood ratio is an optimal decision variable.

CRITERION The set of values of the decision variable that would lead the receiver to decide in favor of the presence of the signal.

HIT RATE The percentage of signal trials on which the receiver would accept the hypothesis that the signal was transmitted (e.g., those trials for which the decision variable falls in the criterion set).

FALSE ALARM RATE The percentage of no-signal trials on which the receiver would accept the hypothesis that the signal was transmitted.

RECEIVER OPERATING CHARACTERISTIC (ROC CURVE) The graphical display of hit rate on the ordinate versus false alarm rate on the abscissa that the receiver would achieve if it made a decision on each trial based upon the decision variable, as to whether or not the signal had been transmitted. The ROC curve depends strongly upon the nature of the receiver, upon the system under study, and upon the conditions of stimulation including parameters of the signal.

MEASURED DISTRIBUTIONS The two frequency distributions of the decision variable as recorded on many repetitions of signal and no-signal trials.

UNDERLYING DISTRIBUTIONS Hypothesized distributions of physiological or physical parameters located in or before the sensory system and distal to the measurement. Underlying distributions are most usefully defined at the site where the dominant noise in the experiment originates. These distributions are precursors of the measured distributions. Often, the purpose of an experiment is to test hypotheses concerning possible underlying distributions.

LIKELIHOOD RATIO A statistic that is defined as the quotient of the probabilities of a particular event under two alternative distributions. The likelihood ratio of a particular value of spike count is obtained from the measured distributions of spike count. The likelihood ratio of a physical variable like the number of photons absorbed in the retina would be computed from the physical distributions of that variable.

DETECTABILITY A unidimensional parameter abstracted from a measured ROC curve that quantifies the ability of the signal to lead to detection, detectability, d'_e, is the sensitivity measure of ROC analysis. d'_e is defined as the separation of means of two unit variance gaussian distributions whose ROC curve intersects a measured ROC curve on the negative diagonal (locus of points for which hit rate plus false alarm rate = 1.0). d'_e is zero for a signal that leads to chance performance, just less than 1.5 for a signal detected with 25 % error, and rises to infinity for a signal detected without error.

EFFICIENCY If an external noise exists and is known (cf. Tanner and Clark-Jones, 1960), a maximal detectability, d'_e, for a hypothetical ideal observer can be computed from parameters of the signal and of the noise that obscures it. The theory of signal detectability is the formal theory that leads to such a computation. *Efficiency* is a measure varying from 0.0 to 1.0 that describes the ratio of the energy required to yield the measured detectability for the ideal observer divided by the energy actually required (cf. Tanner and Birdsall, 1958). Computed in this way, efficiency is measured for the combination of system-under-study measurement device, and receiver. Since information passes serially from one to the next, each can exert an effect on overall efficiency. Thus to measure the efficiency of the system-under-study one needs to know the efficiencies of the other two, as well as the overal efficiency.

QUANTUM EFFICIENCY An efficiency measure for the case where the ideal observer is an ideal photodetector (cf. Rose, 1948). It can be thought of as the transmissivity of a filter which, when placed in front of the ideal photodetector, would constrain its performance to the same level as that of a real detector. As defined by

Rose (1948), quantum efficiency is the square of the Tanner-Birdsall efficiency measure.

(C) *Construction of the ROC Curve*

The procedures involved in ROC analysis will be illustrated for an experiment consisting of 184 signal trials and 180 no-signal trials. The presence or absence of a signal was determined at the transmitter by a random number generator adjusted so that the signal appeared on roughly half of the trials. The number of spikes occurring in the 0.7 s after the start of a trial never exceeded six in this experiment. Thus, the raw data can be displayed in a 2 x 7 table as shown in Table I. This table shows, for example, that a spike count of 3 was observed on 37 of the 184 signal trials. This frequency

TABLE I
FREQUENCIES

	Count							
	0	1	2	3	4	5	6	Total trials
Frequencies of joint events								
No signal	56	54	34	20	9	5	2	180
Signal	7	18	37	39	35	39	9	184
Normalized frequencies of joint events								
No signal	56/180	54/180	34/180	20/180	9/180	5/180	2/180	
Signal	7/184	18/184	37/184	39/184	35/184	39/184	9/184	
Cumulative normalized frequencies								
No signal	1.00	0.69	0.39	0.20	0.09	0.04	0.01	
Signal	1.00	0.96	0.86	0.66	0.45	0.26	0.05	

table is converted to a relative frequency table in a familiar way: each entry is divided by its row total with a result as shown. One interprets the entries in this new table as estimates of conditional probabilities, e.g., given that the signal was presented, the estimate of the probability of obtaining a spike count of 3 is 37/184. This table contains two separate conditional probability distributions, the measured distributions. They are shown graphically in Fig. 12.

The task of the receiver as decision maker can be understood by examining the distributions of Fig. 12. Clearly a given measured value of spike count provides only equivocal evidence as to the presence or absence of the signal. But on the average it appears that the larger the spike count the more likely it is that a dimming signal was presented. Assume that the receiver uses spike count as its decision variable. The following procedures relating to the derivation of sensitivity measures rest on the assumption that the decision variable is monotone with its likelihood ratio. According to Fox (see Peterson, et al., 1954), the receiver should use the likelihood ratio of the measured parameter (or, equivalently, a monotone function of likelihood ratio, ac-

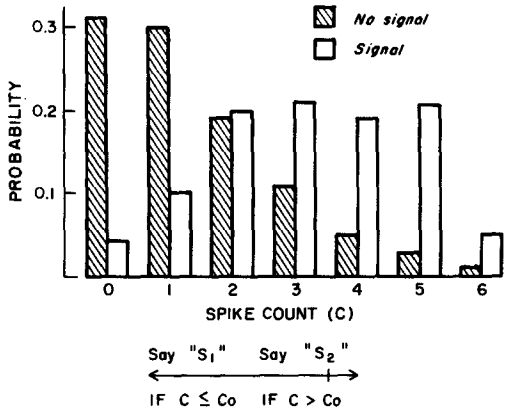

FIGURE 12. Distributions of spike count for signal and no signal. Ordinate: Conditional probability, estimated from relative frequencies of Table I. Abscissa: Spike count. The distributions of response show large variability and considerable overlap. A receiver attempting to decide, based upon spike count, whether or not the signal had been transmitted is constrained to make errors regardless of the decision rule it uses.

cording to Birdsall, 1966) in order to optimize its decisions as to the presence or absence of the signal. In this example, likelihood ratio is the quotient of the two relative frequency entries in a given count column (see Table I). For example, the likelihood ratio for a count of 3 is $37/184 \div 20/180 = 1.91$. Baye's theorem can be used to show that this decision variable, likelihood ratio, equals the posterior odds in favor of the presence of a signal since the prior odds are 1:1.

To verify that spike count is an appropriate decision variable one must determine if spike count is monotone with its likelihood ratio. In the example, likelihood ratio increases in monotone fashion from left to right in the table except for a reversal in the last two entries. All entries in the table are subject to sampling error (see below) and the data from subsequent experiments on this preparation confirm that the likelihood ratio rises monotonically with count, even for those large values of count.

If the receiver were required to make decisions based upon spike count, c it would adopt some realization of the decision rule: if

$$c > c_o$$

decide signal present, otherwise, decide signal absent, because the higher is c, the better the odds in favor of the signal having been sent. This type of decision rule (see below for a derivation) can be realized in different ways depending upon the choice of the criterion cutoff, c_o. The hit rate that the receiver could achieve can be computed as the probability under the measured distribution for signal trials to the right of the cutoff given by c_o. Similarly, the false alarm rate would be the probability under the no-signal distribution to the right of c_o. In Table I the last set of figures shows the relative frequencies of the measured distributions cumulated from the right. As a consequence that table shows in each column a realizable pair of hit rate and false alarm rate. Fig. 13 shows the ROC curve, the plot of possible

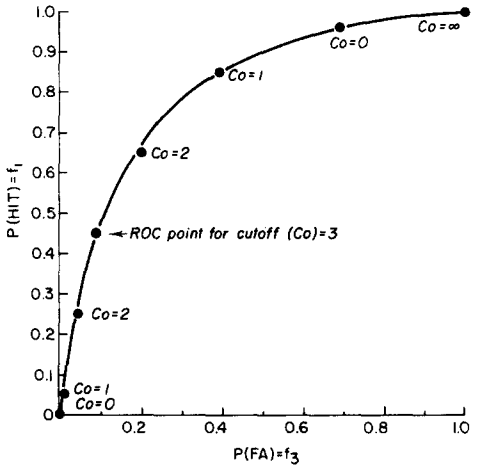

FIGURE 13. ROC curve on linear paper. Ordinate: Hit rate estimated from cumulated relative frequencies given signal. Abscissa: False alarm rate, from cumulated relative frequencies of count given no signal. Each point achieved by adopting a different realization of the decision rule: Say "signal" if count exceeds C_o. With reference to Fig. 12, hit rate and false alarm rate are areas under distributions to the right of C_o.

hit and false alarm rates for various values of c_o. A smooth curve has been drawn through these points. An ROC curve is monotone increasing with monotone decreasing slope for the case of a decision variable monotone with its likelihood ratio. This curve satisfies that ideal except for a slight deviation near the origin, where the slope fails to increase monotonically.

Measure of Sensitivity

The measure of sensitivity used in this paper assesses the extent to which the measured distributions do not overlap. That measure is called detectability and is denoted d'_e. It is defined as the separation of the means of two unit-variance gaussian distributions whose ROC curve intersects the obtained ROC curve at the negative diagonal (line for which hit rate plus false alarm rate = 1.0). d'_e is a measure that rises in monotone fashion with the number of correct decisions. Fig. 14 *a* shows (dashed) two gaussian ROC curves (curves obtained by computation from pairs of equal variance gaussian distributions). The value of the separation of the means of the gaussian distributions in each case is shown as the parameter for each curve. Thus, the sensitivity measure, d'_e, for the measured curve between them is approximately 1.3. The computation of d'_e can be made to any desired precision through the use of tables of the normal deviate (Green and Swets, 1966).

A convenient way to assess detectability is to plot the ROC curve on normal-normal probability paper (Codex 42,453 [Codex Corp., Newton, Mass.] or Keuffel and Esser 47,8062) where the axes are stretched so that equal distances represent the probability increment associated with equal fractions of standard deviation of the normal deviate (z scores). On this paper gaussian ROC curves are straight lines of unit slope. For gaussian distributions of equal variance σ^2, and difference of means, $\Delta\mu$, $d'_e = \Delta\mu/\sigma$.

Unequal variance gaussian distributions produce straight line ROC curves on probability paper also, and the slope is equal to the ratio of the standard deviation in the event no signal is presented to that in the event signal is presented (Green and Swets, 1966).

Fig. 14 *b* shows the ROC curve of Fig. 14 *a* replotted on normal-normal probability paper with *z*-score coordinates also shown. d'_e is read as the vertical axis *z* score less the horizontal axis *z* score. Clearly this *z*-score difference varies over the length of an ROC curve except in the case of an equal variance gaussian ROC curve where it is a constant. For this reason we have adopted the convention of reading the detectability at the negative diagonal.

Bootstrap Procedures for Measuring d'_e of Large Signals

Since high detectability is subject to disproportionately high sampling error (see below), it is worth describing an alternative technique that more accurately quantifies detectability. Bootstrap procedures were introduced in psychophysics (Creelman, 1963; Nachmias and Kocher, 1970). The bootstrap procedure involves experiments on

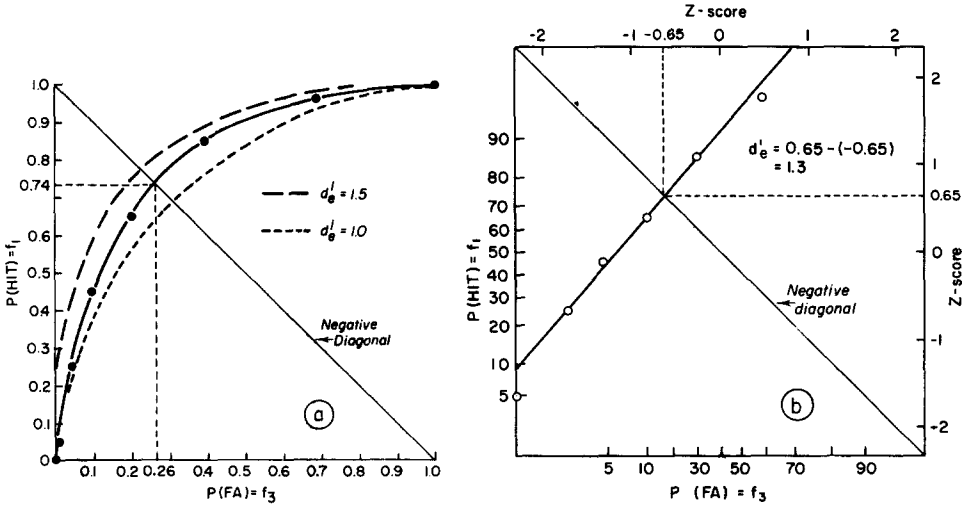

FIGURE 14. (*a*) ROC curve of Fig. 4 plotted with gaussian ROC curves for $d' = 1.5$ (upper) and $d' = 1.0$ (lower). d'_e for empirical ROC curve can be estimated by eye (at the negative diagonal) at about 1.3. d'_e can be measured to any degree of precision using the hit and false alarm rates at the negative diagonal, and tables of the normal deviate. The area under a gaussian distribution to the right of a cutoff which is -0.65 standard deviations from the mean would correspond to the hit rate, 0.74. Likewise, the area to the right of $+0.65$ standard deviations is 0.26. Thus, d'_e is equal to $+0.65 - (-0.65) = 1.3$, the separation of two unit variance gaussian distributions whose ROC curve intersects the measured ROC curve at the negative diagonal. (*b*) Same ROC curve on probability paper (Codex 42453). The intersection of the empirical curve with the negative diagonal has *z*-score coordinates of 0.65 and -0.65. Their difference is d'_e. So $d'_e = 0.65 - (-0.65) = 1.3$. Most ROC curves appear to be fit well by straight lines on probability paper. The slope of the line fitted (by eye) to the curve is 1.19. Therefore, the underlying distribution for signal is presumed to have less variance than that for no signal.

one (or more) additional signal chosen so as to produce effects less than those of the high detectability signal but greater than those due to no signal. Then using the relation

$$d'_e|_n^s = d'_e|_n^{s_1} + d'_e|_{s_1}^s \qquad (1\ a)$$

where $s > s_1$ and where $\frac{j}{i}$ is read "(d'_e) to be evaluated for distributions due to signal conditions i and j," d'_e for the large signal is calculated as the sum of that for the small signal plus the d'_e for discrimination between the two. The validity of Eq. 1 *a* has not been proven except for the case of gaussian equal variance distributions where the proof is trivial, since d'_e is just the normalized separation of means between two distributions. Our computations for Poisson distributions show errors of no more than 1/2 % for Eq. 1 *a*.

Relation of d'_e to the Sensitivity Measures of Other Authors

Two other detectability measures appear in the literature which can be derived from d'_e with additional assumptions. They are compared with d'_e in order to illustrate their limitations. The first has already been mentioned and is due to Fitzhugh (1957). His detectability measure, d, is simply the difference of means of the signal and no-signal spike count distributions. On the assumption that both measured distributions are gaussian with equal variance, and that variance is independent of stimulus conditions, d and d'_e are the same. To understand the limitations of d, consider the analogy of the communication channel. In that analogy, the system under study is considered more sensitive in relation to how well the receiver performs in the task of detecting the presence or absence of a signal. The receiver's performance would increase if the spike count variability decreased. In the limit of zero variance, the performance of the receiver would be perfect. d takes no account of the effects of variance on sensitivity.

Barlow and Levick (1969 *a*) modified Fitzhugh's approach by including the effect of no-signal distribution variance in their definition of threshold. First, the mean and standard deviation of the spontaneous activity were measured and then the mean response for a near-threshold signal was measured. Threshold was defined as the signal energy that moved the mean response a fixed number of standard deviations from the no-signal mean. Two assumptions are implicit here: (*a*) that mean response is linear with signal energy and (*b*) that the variance of the signal distribution equals that of the no-signal distribution. Nakayama (1971) extended their approach to define a detectability, d', as the difference in spike count means divided by the standard deviation of the no-signal distribution. Thus, Nakayama's d' is the same as d'_e providing these distributions are gaussian with equal variance. Nakayama's d' does not take account of the effect which nonlinearities in the system under study can have on the variance of the signal distribution nor does it take account of signal-dependent variance. Both of these factors will affect the decisions that a receiver can make and that influence is reflected only in d'_e.

Statistical Considerations

Since ROC points are obtained from relative frequency estimates of probabilities, they have inherent variance due to sampling error. There are a number of treatments in the

mathematical psychology literature that are relevant to the problems of estimation of parameters of physiological ROC curves (Gourevitch and Galanter, 1967; Dorfman and Alf, 1968; 1969; Ogilvie and Creelman, 1968; and Dorfman et al., 1973). Of special interest are programs that find maximum likelihood estimates of d'_e and ROC slope (cf. Dorfman et al., 1973). An estimate derived from the work of Ogilvie and Creelman (1968) is a useful approximation for the standard error to be expected in d'_e estimated in an experiment of N trials divided equally between signal and no-signal conditions. The estimate is based on the assumption that underlying distributions can be approximated as logistic distributions. Then, SE $(d') = 2.13/N^{1/2}$ providing $d'_e < 2.0$, otherwise standard error rises as a power of d'_e.

(D) *The Concept of the Ideal Observer*

The *ideal observer* (Peterson, 1954) is a mathematical construct that enables the calculation of theoretically optimal performance. It can be used to assess whether or not receiver design is good (Cohn, 1969), and it can be used to compare measured performance to the best possible detection performance for the physical signals in question. If measured performance matches ideal performance then, considering the block diagram of Fig. 2, the system under study, the measurement, and the receiver each must process information relevant to the presence or absence of the signal as efficiently as is possible. In this case, the range of physiological explanations for the performance of the system under study is considerably constrained. If measured performance fails to match ideal performance then the way in which it has failed may provide clues as to the function of the system under study. The difference between ideal and measured performance is quantified by the concept of efficiency (see Terminology). The experimenter must be careful not to mistake inefficiency in the measurement and/or the receiver for inefficiency in the system under study.

Receiver inefficiency, and its possible dependence upon stimulus conditions, are topics that have not yet received a thorough analysis. Fitzhugh (1957) and Barlow and Levick (1969 *a*) showed that the design of the receiver can exert a strong influence on the conclusions one draws from an experiment. Therefore the experimenter must be cautious in the choice of a receiver. This caution is no less important in studies not utilizing ROC analysis.

Example 1: Gaussian Noise Limit (Tanner and Clark-Jones, 1960)

The performance of the ideal observer is defined in terms of the signal at the transmitter and the noise there that obscures it. The case for gaussian noise is useful to review because it is applicable in many situations and because it is a good approximation in the Poisson case which is of interest in the present paper. Consider the example of a signal that is a decrement of a fixed luminance target of area A and duration, T, where T is less than the integrating time of the eye being studied. Let the amplitude of the decrement be E and the background luminance be B. Suppose that the background luminance fluctuates randomly (but not necessarily due to quantum effects) with a distribution that is gaussian with zero mean, and with variance N^2. Then the input, x, to an observer is a gaussian random variable. When a signal is sent, the mean is $(B - E)$ and the variance is N^2. When no signal is sent, the mean is B and variance

is N^2. Let $f_s(s)$ be the probability distribution of the input when a signal is sent and $f_N(x)$ be the distribution when no signal is sent. These are the underlying distributions in this example.

The optimal performance in any noise-limited situation may be calculated as follows (specific assumptions about the distribution of the noise are introduced only after Eq. 4). The ideal observer is defined as the observer that maximizes the quantity, M:

$$M = \Pr(\text{HIT}) - w \Pr(\text{FA}), \tag{2 a}$$

where w is a constant that specifies the relative importance of hits and false alarms. Eq. (2 *a*) embodies assumption *d* on p. 604 above.

Hit and false alarm rates are defined by

$$\begin{aligned} \Pr(\text{HIT}) &= \int_c f_s(x)\,dx, \\ \Pr(\text{FA}) &= \int_c f_n(x)\,dx, \end{aligned} \tag{3 a}$$

where c is the set of all x such that the decision of the observer is that the signal was sent.

The decision problem then becomes one of maximizing

$$M = \int_c (f_s(x) - w f_n(x))\,dx,$$

which occurs when c is the set of all values of x such that $f_s(x) - w f_n(x) > 0$ because then every x contributes a positive increment to the integral.

Thus

$$\frac{f_s(x)}{f_N(x)} \geq w \tag{4 a}$$

defines the criterion, c. The quantity $f_s(x)/f_N(x)$ is the likelihood ratio. If the likelihood ratio of a given input, x, exceeds w, the ideal observer decides in favor of the signal. In the present case the noise has been assumed to be gaussian. It can be shown (Green and Swets, 1966) that the gaussian random variable, x, is monotone with its likelihood ratio so x is also an optimal decision variable and the decision rule becomes: say yes if

$$x \geq x_o, \tag{5 a}$$

where

$$\frac{f_s(x_0)}{f_N(x_0)} = w.$$

Thus, this decision problem is represented by two gaussian distributions with separation E and standard deviation, N. Then for the ideal observer d'_e is

$$d'_e = \frac{\Delta \text{ means}}{\text{SD}} = \frac{E}{N}, \tag{6 a}$$

and gaussian ROC curves are predicted. Eq. 6 *a* is applicable if and only if gaussian distributions of equal variance define the decision problem.

Quantum Efficiency

The way in which measured performance fails to achieve ideal performance can provide clues as to the underlying physiology. Suppose, for example, that the frog retina behaved in an ideal manner except that it failed to catch a fraction, $1 - F$, of the incident photons. Then, to match the performance of the system under study, the formulation of the ideal observer can be degraded by assuming the existence of a filter of transmissivity, F, placed in front of the ideal observer. Eq. 3 is repeated

$$d'_e = \frac{FEAT}{(FBAT)^{1/2}}, \tag{7 a}$$

and F is the quantum efficiency of the degraded ideal observer.

Quantum efficiency can be measured directly, if E, B, A, and T, are known, by calculating E', the energy of the signal delivered to an ideal observer so as to satisfy the requirement that the performance of the ideal observer equals the performance of the real observer.

Thus,

$$\frac{FEAT}{(FBAT)^{1/2}} = \frac{E'AT}{(BAT)^{1/2}}, \tag{8 a}$$

or

$$F = \left(\frac{E'}{E}\right)^2.$$

It should be noted that Eq. 8 *a* involves an approximation which, in the case of decrement signals, underestimates attainable d'_e. Therefore, calculations of F tend to be slight overestimates, but can never be wrong by more than a factor of 2.0 Table II shows how large the error can be for selected values of BAT and d'_e.

TABLE II

PERCENT BY WHICH d'_e CALCULATED FROM EQ. 8 *a* IS UNDERESTIMATED DUE TO GAUSSIAN APPROXIMATION

	BAT		
d'_e	4	12	36
	%	%	%
1.0	15	13	5
2.0	26	18	10
3.0		26	14

We thank H. B. Barlow for reading an early version of the manuscript, Janis Miyamoto-Mills for typing the manuscript, and Gloria Pelatowski for drafting figures.
Research was supported in part by NIGMS Training Grant NIH SP01 GM 01289 to T.E.C., by NIH Grant EY00379 to D.G.G., and by contract F44620-68-C-0090 from the Air Force Office of Scientific Research to W.P.T.

Received for publication 23 December 1974.

REFERENCES

ADRIAN, E. O., and R. MATTHEWS. 1928. The action of light on the eye. Part 3. The interaction of retinal neurons. *J. Physiol. (Lond.)*. **65**:273–298.

BARLOW, H. B. 1964. The physical limits of visual discrimination. *In* Photophysiology. A. C. Geise, editor. Academic Press, Inc., New York. **2**: Chap. 16.

BARLOW, H. B. 1965. Optic nerve impulses and Weber's Law. *Cold Spring Harbor Symp. Quant. Biol.* **30**:539–552.

BARLOW, H. B., and T. E. COHN. 1971. Quantum fluctuations and the variability of spike discharge in the cat. Paper presented at Annual Meeting of Association for Research in Vision and Ophthalmology. Sarasota.

BARLOW, H. B., and W. R. LEVICK. 1969 *a*. Three factors limiting the reliable detection of light by retinal ganglion cells of the frog. *J. Physiol. (Lond.)*. **200**:1–24.

BARLOW, H. B., and W. R. LEVICK. 1969 *b*. Changes in the maintained discharge with adaptation level in the cat retina. *J. Physiol. (Lond.)*. **202**:699–718.

BARLOW, H. B., W. R. LEVICK, and M. YOON. 1971. Responses to single quanta of light in retinal ganglion cells of the cat. *Vis. Res.* (Suppl. 3) 87–101.

BIRDSALL, T. G. 1966. The ROC curve and its character. Ph.D. Thesis. University of Michigan. University Microfilms, Ann Arbor, Michigan. Order number 67-08217.

COHN, T. E. 1969. Theory of signal detectability: Application to the study of the activity of single cells of the frog visual system. Ph.D. Thesis. University of Michigan. University Microfilms, Ann Arbor, Michigan. Order number 70-21630.

COHN, T. E. 1974. A new hypothesis to explain why the increment threshold exceeds the decrement threshold. *Vis. Res.* **14**:1277–1279.

COHN, T. E., L. N. THIBOS, and R. KLEINSTEIN. 1974. The detectability of a luminance increment. *J. Opt. Soc. Am.* **64**:1321–1327.

CREELMAN, C. D. 1963. Detection discrimination, and the loudness of short tones. *J. Acoust. Soc. Am.* **35**:1201–1205.

CRESCITELLI, F. 1958. The natural history of visual pigments. *Ann. N.Y. Acad. Sci.* **74**:230–254.

DENTON, E. J., and M. H. PIRENNE. 1954. The visual sensitivity of the toad *Xenopus laevis*. *J. Physiol. (Lond.)*. **125**:181–207.

DENTON, E. J., and J. H. WYLLIE. 1955. Study of the photosensitive pigments in the pink and green rods of the frog. *J. Physiol. (Lond.)*. **127**:81–89.

TEN DOESSCHATE, J. 1958. Differential threshold and firing probability of the off-effect in the frog retina. *Ophthalmologica*. **135**:301–307.

DONNER, K. O., and T. REUTER. 1968. Visual adaptation of the rhodopsin rods in the frog's retina. *J. Physiol. (Lond.)*. **199**:59–87.

DORFMAN, D. D., and E. ALF. JR. 1968. Maximum-likelihood estimation of parameters of signal-detection theory—A direct solution. *Psychometrika*. **33**:117–124.

DORFMAN, D. D., and E. ALF. JR. 1969. Maximum-likelihood estimation of parameters of signal-detection theory and determination of confidence intervals—Rating method data. *J. Math. Psychol.* **6**:487–496.

DORFMAN, D. D., L. L. BEAVERS, and C. SASLOW. 1973. Estimation of signal detection theory parameters from rating scale data: A comparison of the method of scoring and direct search. *Bull. Psychon. Soc.* **1**:207–208.

FAIN, G. 1975. Quantum sensitivity of rods in the toad retina. *Science (Wash. D.C.)*. **187**:838–841.

FITZHUGH, R. 1957. The statistical detection of threshold signals in the retina. *J. Gen. Physiol.* **40**:925–948.

GESTELAND, R. C., B. HOWLAND, J. Y. LETTVIN, and W. H. PITTS. 1959. Comments on microelectrodes. *Proc. IRE.* **47**:1856–1862.

GOUREVITCH, V., and E. GALANTER. 1967. A significance test for one parameter isosensitivity functions. *Psychometrika.* **32**:25–33.

GRANIT, R. 1955. Receptors and Sensory Perception. Yale University Press, New Haven, Conn.

GREEN, D. G. 1969. Sinusoidal flicker characteristics of the color-sensitive mechanisms of the eye. *Vis. Res.* **9**:591–601.

GREEN, D. G., and F. MAASEIDVAAG. 1967. Closed-circuit television pupilometer. *J. Opt. Soc. Am.* **57**:830–833.

GREEN, D. M., and J. A. SWETS. 1966. Signal Detection Theory and Psychophysics. John Wiley & Sons, New York.

HECHT, S., S. SHLAER, and M. P. PIRENNE. 1942. Energy quanta and vision. *J. Gen. Physiol.* **25**:819–840.

JACOBS, G. H. 1972. Spontaneous activity in visual systems. *Am. J. Opt.* **49**:905–921.

KAPLAN, H. M. 1967. Anesthesia in amphibians and reptiles. *Fed. Proc.* **28**:1541–1546.

KENNEDY, D., and R. D. MILKMAN. 1956. Selective light absorption by the lenses of lower vertebrates and its influence on spectral sensitivity. *Biol. Bull. (Woods Hole).* **111**:375–386.

LEGRAND, Y. 1968. Light, Colour, and Vision. Chapman and Hall, London. 2nd Edition.

LIEBMAN, P., and G. ENTINE. 1967. Cyanopsin—a visual pigment of retinal origin. *Nature (Lond.).* **216**:501–503.

LIEBMAN, P., and G. ENTINE. 1968. Visual pigments of frog and tadpole (*Rana pipiens*). *Vis. Res.* **8**:761–775.

LOWRY, E. F. 1952. Physical basis for some aspects of fluorescent lamp behavior. *Illum. Eng. (New York).* **47**:639–644.

MATURANA, H. R., J. Y. LETTVIN, W. H. PITTS, and W. MCCULLOCH. 1960. Physiology and anatomy of vision in the frog. *J. Gen. Physiol.* **43**:385–404.

MOORE, G. P., D. H. PERKEL, and J. P. SEGUNDO. 1966. Statistical analysis of neuronal spike data. *Ann. Rev. Physiol.* **28**:493–522.

NACHMIAS, J., and E. C. KOCHER. 1970. Visual detection and discrimation of luminance increments. *J. Opt. Soc. Am.* **60**:382–389.

NAKAYAMA, K. 1971. Local adaptation in cat LGN cells: evidence for a surround antagonism. *Vis. Res.* **11**:501–509.

OGILVIE, J. C., and C. D. CREELMAN. 1968. Maximum-likelihood estimation of receiver operating characteristic curve parameters. *J. Math. Psychol.* **5**:377–391.

PETERSON, W. W., T. E. BIRDSALL, and W. C. FOX. 1954. The theory of signal detectability. *Trans. IRE P.G.I.T.*, **4**:171–212.

RATLIFF, F., H. K. HARTLINE, and D. LANGE. 1968. Variability of interspike intervals in optic nerve fibers of *Limulus*: Effect of light and dark adaptation. *Proc. Natl. Acad. Sci. U.S.A.* **60**:464–469.

REICHARDT, W. E. 1966. Detection of single quanta by the compound eye of the fly, *Musca*. The Functional Organization of the Compound Eye. C. G. Bernhard, editor. Pergamon Press, Inc., Elmsford, N.Y. **7**:267–290.

ROSE, A. 1948. The sensitivity performance of the human eye on an absolute scale. *J. Opt. Soc. Am.* **38**:196–208.

ROSENBLITH, W. A. 1962. Processing Neuroelectric Data. The M.I.T. Press, Cambridge, Mass.

SAKITT, B. 1972. Chanting every quantum. *J. Physiol. (Lond.).* **223**:131–150.

TANNER, W. P. JR. 1961. Physiological implications of psychophysical data. *Ann. N. Y. Acad. Sci.* **89**:752–765.

TANNER, W. P., JR., and T. G. BIRDSALL. 1958. Definitions of d' and η as psychophysical measures. *J. Acoust. Soc. Am.* **30**:922–928.

TANNER W. P., JR., and R. CLARK-JONES. 1960. The ideal sensor system as approached through SDT and TSD. *In* Visual Search Problems. A. Morris and E. P. Horne, editors. Armed Forces—NRC Committee on Vision. NAS-NRC Publication # 712. Washington.

TANNER, W. P., JR., and J. A. SWETS. 1954. A decision-making theory of visual detection. *Psychol. Rev.* **61**:401–409.

VERVEEN, A. A., and H. E. DIRKSEN. 1965. Fluctuations in membrane potentials of axons and the problem of coding. *Kybernetik.* **2**:152–160.

DEVRIES, H. 1943. The quantum character of light and its bearing upon the threshold of vision, the differential sensitivity and the visual acuity of the eye. *Physica (Utrecht).* **10**:553–564.

WALL, P. D. 1959. Repetitive discharge of neurons. *J. Neurophysiol.* **22**:305–320.

YEANDLE, S. 1958. Evidence of quantized slow potentials in the eye of *Limulus*. *Am. J. Ophthalmol.* **46**:82–87.